UDC 577.32

LIGAND-BINDING SITES ON THE *MYCOBACTERIUM TUBERCULOSIS* UREASE
Lisnyak Yu. V., Martynov A. V.

**Mechnikov Institute of Microbiology and Immunology**

Introduction

Mycobacterium tuberculosis is the causative agent of tuberculosis that remains a serious medical and social health problem now [1]. Despite intensive efforts have been made in the past decade, there are no new efficient anti-tuberculosis drugs today, and that need is growing due to the spread of drug-resistant strains of *M.tuberculosis* [2].

Mycobacterium tuberculosis urease (MTU), a representative of a group of nickel-dependent metalloenzymes (urea amidohydrolase, EC 3.5.1.5) [3-6]

produced by various bacteria [7-11], fungi [8, 12], and plants [7, 8, 13]. Bacterial ureases have gained much attention as a virulence factor in human and animal infections [14-17]. Bacterial ureases are multimers of three-subunits (except Helicobacter pylori which comprises two-subunits), α-, β- and γ-chains, which form a heterotrimer αβγ. Three αβγ heterotrimers form quaternary complex $(\alpha\beta\gamma)_3$, homotrimer of heterotrimers (fig. 1). The active site containing two Ni atoms is situated in the α-subunit and is flanked by a flexible flap. The flap have been shown to exist in closed, open and wide-open conformations, respectively closing, opening and wide-opening access to the active site, and thus playing a key role in the control of urease activity [18-21].

MTU catalyses the hydrolysis of urea to get ammonia and carbamate which then decomposes with water to get ammonia and carbon dioxide. The consequence of these catalytic reactions is an increase of pH (i.e. alkalinizing of
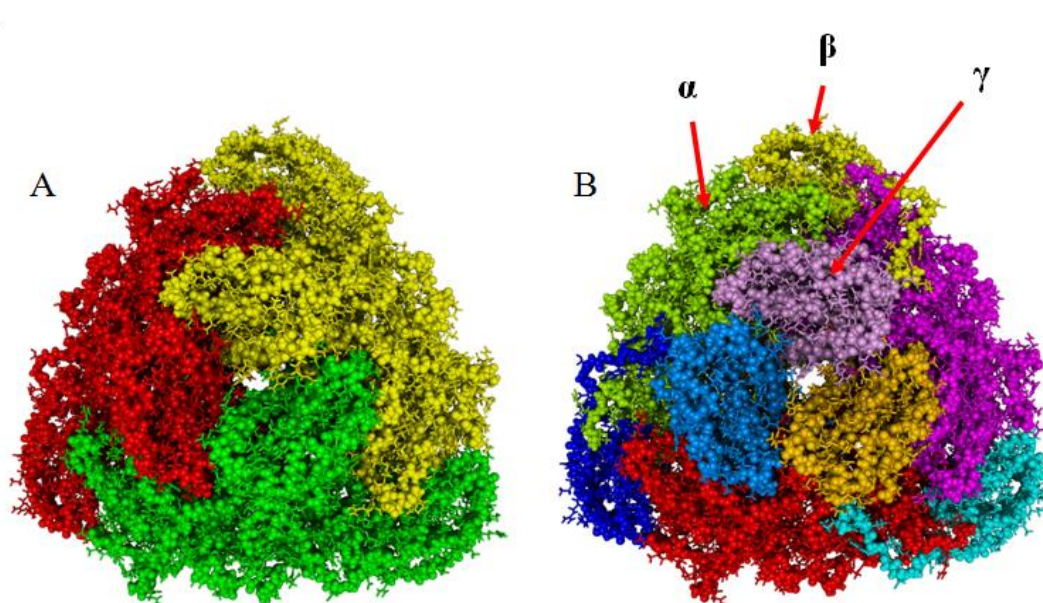
Fig. 1 – Structure of bacterial urease. A – homotrimer of heterotrimers $(\alpha\beta\gamma)_3$. The homotrimers αβγ are represented in different colors. B – sub-unit structure of the homotrimer of heterotrimers $(\alpha\beta\gamma)_3$. In each heterotrimer, α, β and γ sub-units are represented in different colors.

the environment) that is skillfully used by pathogenic bacteria for their comfortable survival within the host organism [22]. Thus, *M. tuberculosis* urease, being an important factor of the bacterium viability and virulence, is an attractive target for anti-tuberculosis drugs acting by inhibition of urease activity. However, the commercially available urease inhibitors, such as phosphorodiamidates, hydroxamic acid derivatives and imidazoles are toxic and unstable, that prevent their clinical use [23-25]. Therefore, new more potent anti-tuberculosis drugs inhibiting new targets are urgently needed. A powerful tool for the search of novel inhibitors is a computational drug design [26-27]. The inhibitor design is significantly easier if binding sites on the enzyme are identified in advance [28]. This paper aimed to determine the probable ligand binding sites on the surface of *M. tuberculosis* urease.

DOI: 10.5281/zenodo.1000136

Methods

Homology model of Mycobacterium tuberculosis urease. In the absence of experimental structure of MTU, to search the potential ligand-binding sites on the enzyme's surface there was used MTU homology model built by us earlier [29]. Briefly, the target amino acid sequence of *Mycobacterium tuberculosis* H37Rv urease was retrieved from GenBank at NCBI [30]. Potential modeling templates were identified by runninig PSI-BLAST [31, 32] to extract a position-specific scoring matrix from UniRef90 and then searching the PDB [33] for a match with the target sequence. The templates were ranked based on the alignment score and the structural quality according to WHAT_CHECK [34] obtained from the PDBFinder2 database [35]. Amongst the top-scoring templates, five high-resolution X-ray structures were selected for

Klebsiella aerogenes, *Sporosarcina pasteurii,* and *Enterobacter aerogenes* bacterial ureases with three-subunit composition: 2KAU, 5G4H, 4UBP, 4CEU, and 4EPB. For each template five stochastic alignments were created [36] using SSALIGN scoring matrices [37]. Then for each alignment, a three-dimensional model was built using loop conformation extracted from the PDB [38] and the SCRWL side-chain placement algorithm [39]. Hydrogen bonding network was optimized [40]. Each model was energy minimized with explicit water molecules using Yasara2 force field [41], and the models were ranked by quality Z-score. The best scoring model was further refined by running a 500 ps molecular dynamics simulation using Yasara2 force field. During the simulation, snapshots were saved every 25 ps and rated according to the quality Z-score. The model with highest quality score was chosen as a final homology model of 3D structure for *M. tuberculosis* urease.

Mapping of M. tuberculosis urease surface by FTSite. To identify ligand binding sites on MTU surface, computational solvent mapping algorithm FTSite was applied through the online server [42, 43]. The FTSite method is based on the concept of "hot spots", the regions of protein binding sites that are major contributors to the binding free energy and, hence, are prime targets in drug design [42-45]. The method places molecular probes - small organic molecules containing various functional groups – on a dense grid defined around the protein, and for each probe finds favorable positions by rigid body search using empirical free energy functions. This step uses the fast Fourier transform correlation approach to sample billions of probe positions on translational and rotational grids, consisting of 0.8 Å translations and of 500 rotations at each location. Further, the selected poses are refined by free energy minimization using the more accurate free energy potential, the low energy conformations are clustered, and the clusters are ranked on the basis of the average free energy [28, 42, 43]. To determine the hot spots, there are found consensus sites (CSs), i.e. regions on the protein that bind several different probe clusters, and these sites are ranked by the number of nonbound contacts between the protein and all probes in the consensus cluster. The consensus cluster with the highest number of contacts is ranked first; nearby consensus clusters are also joined with this cluster. The amino acid residues in contact with the probes of this newly defined cluster constitute the top ranked predicted ligand binding site. Clusters with fewer contacts define lower ranked predictions [43]. The 16 probe molecules that represent fragments of drug molecules with diverse hydrophobic and hydrophilic properties are benzene, cyclohexane, ethane, ethanol, isopropanol, isobutanol, acetone, acetaldehyde, dimethyl ether, acetonitrile, urea, methylamine, phenol, benzaldehyde, acetamide and N, N-dimethylformamide. To evaluate the clusters of bound probe molecules, there were used energy functions that account for nonbonded van der Waals and electrostatic interactions, as well as solvation effects [28, 42, 43]. FTSite server outputs the protein residues delineating a binding sites and the probe molecules representing each cluster in a consensus site.

Mapping of M. tuberculosis urease surface by AlloPred and AlloSite. AlloPred is a novel method to predict allosteric pockets on proteins [46] which uses the normal mode analysis (NMA) [47]. AlloPred models how the dynamics of a protein would be altered in the presence of a modulator at a specific pocket. This method assumes nothing about the shape of the modulator, and determines only how it affects the flexibility of the whole pocket to which it binds. Pockets on the protein were first predicted using the Fpocket algorithm [48], which locates pockets using Voronoi tessellation and alpha spheres. The normal modes of the protein were then calculated using the elastic network model [49], except the spring constant of any atom pair including a residue in a chosen pocket was set to be a higher value. To model the reduction in flexibility of allosteric pocket on modulator binding, the unperturbed normal modes were first calculated for the protein. The calculation was then repeated, each time perturbing one of the pockets in the protein. These results were combined with output from Fpocket in a support vector machine (SVM) to predict allosteric pockets on proteins. AlloPred is available through a web server [46].

The AlloSite server [50] is similar to the AlloPred method in that it uses the Fpocket algorithm to elucidate allosteric pockets, whereas AlloPred uses an approach that combines flexibility with the Fpocket output. A combination of methods may give better predictions than either method individually [46].

Results and discussion

Homology model of M. tuberculosis urease. Homology model of MTU is a nonamer consisting of 2349 residues (fig. 2). Three subunits of MTU (α, β, and γ) form a quaternary complex, heterotrimer αβγ. Three αβγ heterotrimers form homotrimer of heterotrimers (αβγ)₃. To distinguish between different heterotrimer's chains (αβγ) in the homotrimer, the chains are further denoted as CBA, FED, and IHG for $\alpha_1\beta_1\gamma_1$, $\alpha_2\beta_2\gamma_2$, and $\alpha_3\beta_3\gamma_3$ heterotrimers, accordingly [30]. Subunit α contains the enzyme active site at the bottom of deep channel flanked by a mobile flap comprised of residues 524-545 that includes two α-helices and a flexible loop between them. In our model, the flap is in closed conformation. The channel into the active site's binding pocket lies on the border between two subunits, the third subunit is situated on the other side of the channel from the flap.

Ligand-binding sites on the surface of M. tuberculosis urease. FTSite server outputs only three top ranked probable binding sites. Binding sites 1, 2 and
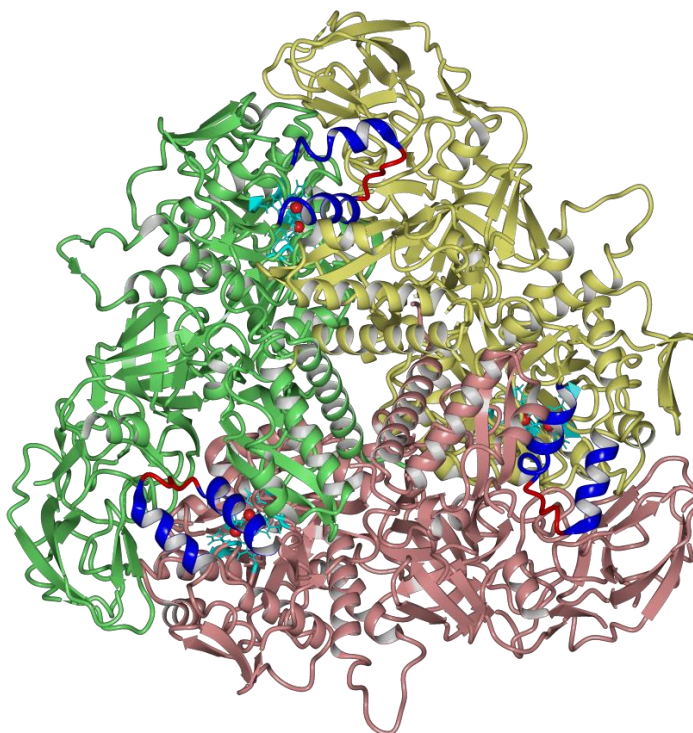
Fig. 2 –Structure of MTU homotrimer of heterotrimers (αβγ)₃. Heterotrimers, CBA, FED, and IHG, are colored in green,   yellow and pink, respectively. The flaps consist of two α-helices (blue) and a flexible loop (red). Ni atoms and their coordinated residues are red- and cyan-colored, respectively

.

3 identified by FTSite on the nonamer *M. tuberculosis* urease structure are described in Table 1 and shown in figs. 3 and 4. Site 1 contains probe clusters of acetamide, cyclohexane and ethane, while site 2 contains cyclohexane, acetone, benzaldehyde, benzene, *tert*-butanol, dimethyl ether, phenol, N,N-dimethylformamide, and isopropanol clusters. Site 3, being a symmetrical equivalent of sites 1 and 2 (fig. 3 and 4), contains probe clusters identical with ones in site 2 and acetonitrile as well. Site 2 is joined to site 1, and their probe clusters are very close to each other indicating the potentially more extended ligand binding site. Interestingly, the top ranked predictions are very close to the entrance of deep pocket (fig. 5 A-C). The clustering of small molecular probes in such regions may suggest that the amino acid residues involved are likely the

Table 1. Probable binding sites on *M. tuberculosis* urease identified by FTSite.

| Site	Description	Surrounding residues
1	Situated at the interface between chains C and A, and chain G of neighbour trimer.	Met 1G, Arg 2G, His 32A, Ile 36A, Phe 655C, Gln 685C, Val 687C
2	Similarly to site 1, situated at the interface between chains C and A, but closer to the active center than site 1.	Leu 77A, Glu 79A, Val 80A, Gln 81A, Thr 683C, Pro 684C, Gln 685C
3	Situated in the symmetrical trimer. Contains only residues equivalent to ones in sites 1 and 2.	Arg 2D, Ile 36D, Glu 79D, Val 80D, Gln 81D, Thr 683F, Pro 684F, Gln 685F, Val 687F

* - Residues that coincide with ones of ancillary pocket are underlined.
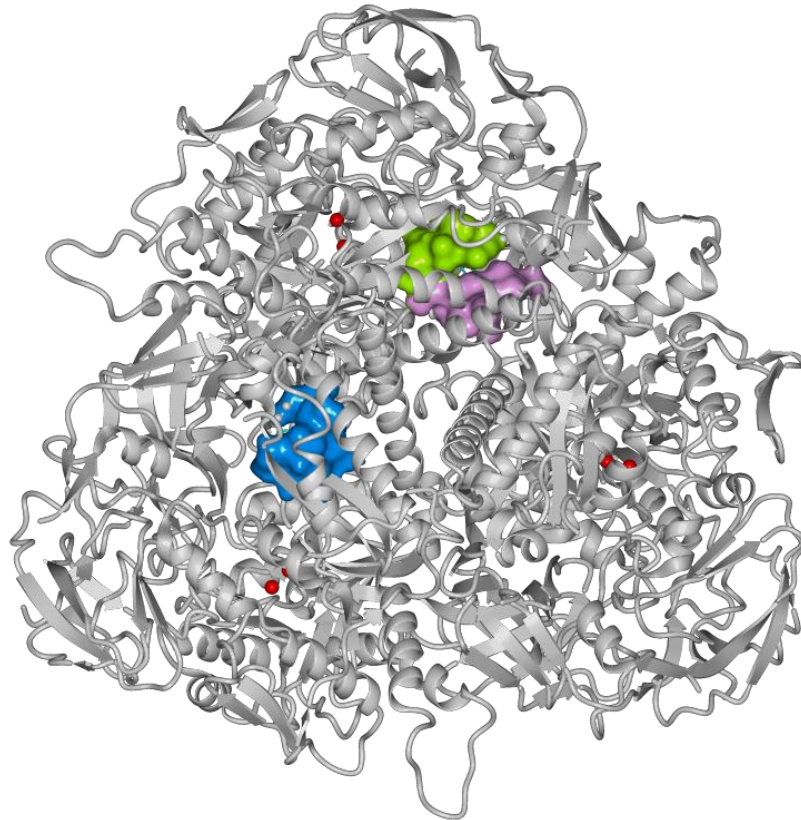
Fig. 3 - Binding sites of *M. tuberculosis* urease identified by FTSite: sites 1, 2 and 3 are colored in pink, chartreuse-green and light-blue, respectively. Ni atoms are colored in red.
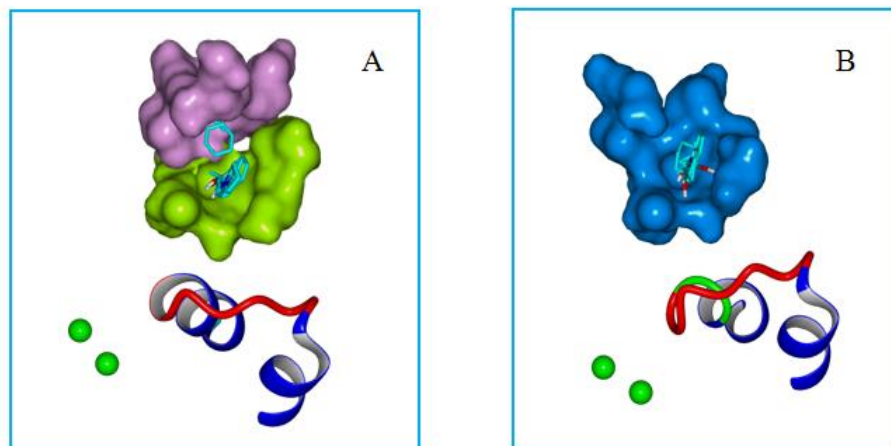
Fig. 4 – Enlarged view at MTU binding sites identified by FTSite. A – Sites 1 and 2 with consensus clusters of bound probes, the flap and Ni atoms. B – Site 3 with consensus clusters of bound probes, the flap and Ni atoms. Sites 1, 2 and 3 are colored in pink, chartreuse-green and light-blue, respectively. Atoms of probe molecules are colored in cyan (carbon), blue (nitrogen), red (oxygen), and white (hydrogen). Ni atoms are colored in green, the flap is colored in red (turn) and blue (helixes).
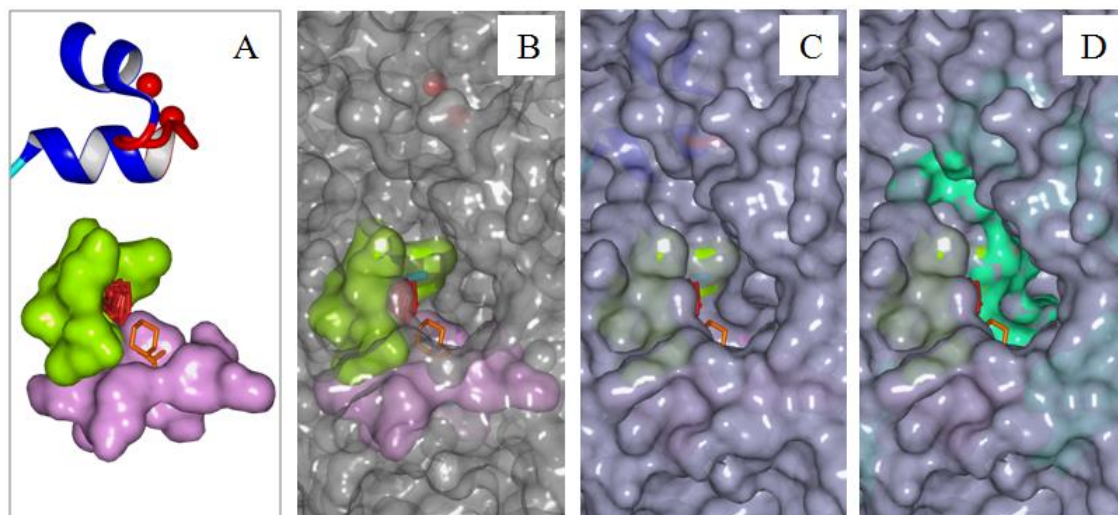
Fig. 5 – Enlarged view at MTU binding sites 1 and 2 and their location in the binding pocket (MTU structure is hidden for clarity). A – Sites 1 and 2 with consensus clusters of bound probes, as well the flap and Ni atoms. B – D – the same as in A and MTU molecular surface: B – surface transparency 75 %, D – overlapping of the surfaces of ancillary pocket and of entrance to the deep binding pocket. Sites 1 and 2 are colored in pink and chartreuse-green, respectively. Consensus clusters of probes are colored in orange (site 1) and red-orange (site 2). Ni atoms are colored in red, the flap is colored in blue (helixes) and red (turn). Ancillary pocket's surface is cyan colored.

intermediate binding sites to be responsible for recruiting a ligand to the binding site deeply buried in the protein [28, 42, 53]. In nonamer MTU structure, three top ranked binding sites revealed by FTSite are beyond the enzyme's active sites (Table 1, fig. 3 and 4). Similar results were observed while FTSite mapping of experimental Protein Data Bank structures of ureases having flaps in closed conformation as well as MTU (2KAU, *Klebsiella aerogenes* urease, and 3UBP, *Sporosarcina aerogenes* urease). When we similarly mapped the PDB structures of

ureases with open flaps, the three top ranked binding sites were located exactly in the three active sites of urease nonamer as for example in 2UBP structure of *Sporosarcina aerogenes* urease shown in fig. 6 (compare with fig. 3).

Fig. 6 - Binding sites of *Sporosarcina aerogenes* urease (2UBP) identified by FTSite: sites 1, 2 and 3 are colored in pink, chartreuse-green and light-blue, respectively.
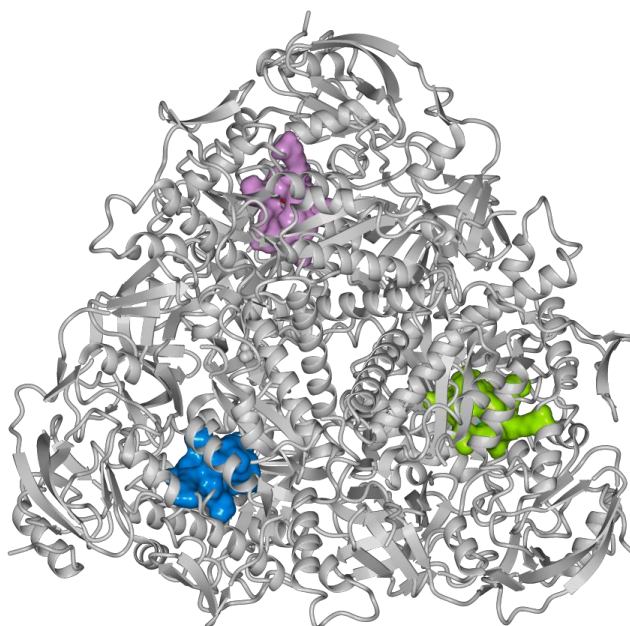
The result is expectable because the enzyme's active sites are known to be the sites of the most tight ligand binding, and these binding sites are accessible while the flap is open. When the flap closes the binding pocket, the ligand binding can occur on the other sites of enzyme. It is interesting in this regard that recently Roberts B. P. et al. noted a region of *Klebsiella aerogenes* urease binding pocket, an ancillary pocket, which remains open and, consequentally, solvent exposed even while the flap is closed [19]. The function of this pocket was unknown, and the authors hypothesized that it may be a substrate/product reservoir (an analogue of the above "intermediate binding" site [28, 42]) or a site for allostery binding. By comparing the structure and sequence of *K.aerogenes* urease with three other ones from *H. pilori*, *Bacillus. pasteurii*, and jack bean, Roberts B. P. et al. found that the ancillary pocket exists in all four ureases and the amino acid residues of ancillary pocket are less conserved, on average, than in the enzyme at large and in particular in the flap, which is more highly conserved. The later feature of ancillary pocket's residues is characteristic for allosteric sites which may represent a novel drug target being more diverse and, consequently more selective than classic orthosteric sites [51, 52]. The allosteric sites hold especial interest since our preliminary studies indicated the possibility to develop supramolecular inhibitors which are not the substrate inhibitors of urease (unpublished). So we compared the locations of MTU ancillary pockets and binding sites 1, 2 and 3 revealed by FTSite and found that the binding sites on MTU partially overlap with its ancillary pockets (fig. 7 and Table 1). Sites 1 and 2 comprise 3 and 2 residues of ancillary pocket, respectively. Site 3 comprises 3 ancillary pocket's residues which are equivalent to ones in sites 1, 2. As can be seen from fig. 5D, the probe clusters of sites 1 and 2 are located at ancillary pocket too. To further explore whether the revealed MTU binding sites may be the potential allosteric sites, we carried out the search for probable sites of allostery binding on MTU surface by AlloPred and AlloSite servers. The results of the search by AlloPred are presented in Table 2 and fig. 8. Predicted allosteric site 0 (in accord with AlloPred's output numbering) consists of 39 residues. It contains 2 residues
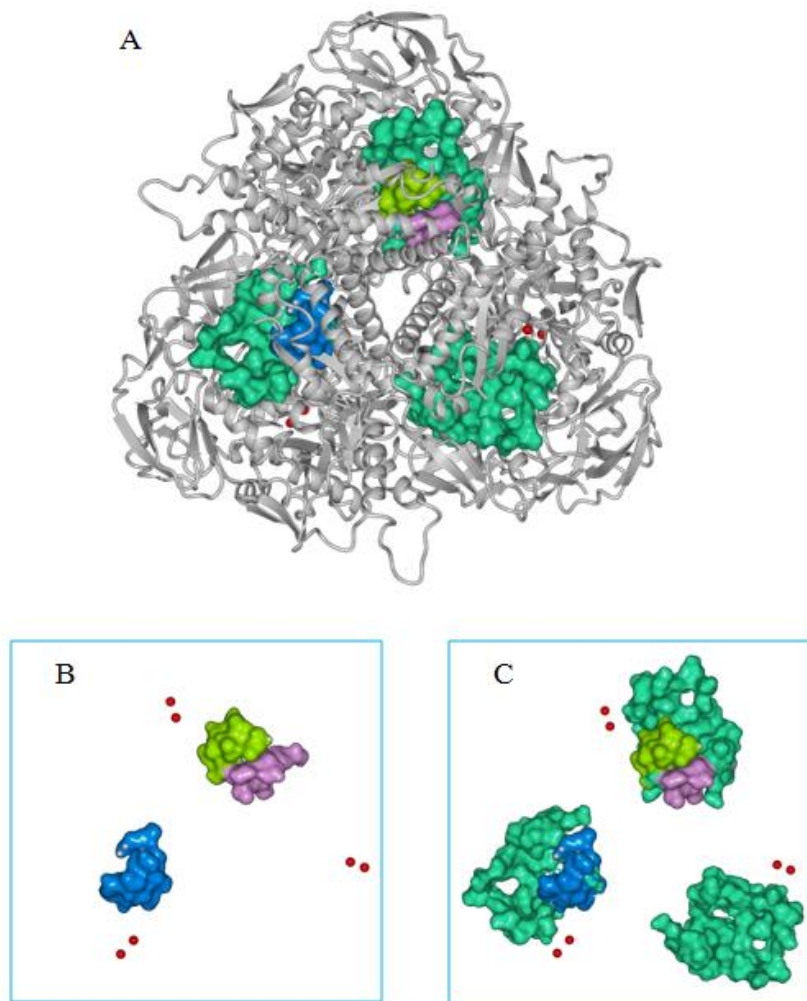
Fig. 7 - Binding sites (identified by FTSite) and ancillary pockets of *M. tuberculosis* urease. A - Binding sites 1, 2 and 3 (colored in pink, chartreuse-green and light-blue, respectively) and ancillary pockets (colored in cyan). Active site's Ni atoms are colored in red. B, C – Shown separately, binding sites 1-3 and Ni atoms (B), and binding sites 1-3, Ni atoms and ancillary pockets (C). (MTU structure is hidden for clarity)

which are equivalent to ones of FTSite's site 1 and 1 residue common with ancillary pocket. Next site 1 is

ommited in Table 2 since it is situated around the central hole of MTU nonamer far from sites of our interest and appear to

Table 2. Probable allosteric sites of *M. tuberculosis* urease identified by AlloPred

Site*	Description	Surrounding residues
0	Situated at the interface between the chain F and chains A and C of neighbour trimer.	**Arg 2A****, Leu 3A, Thr 4A, Pro 5A, His 6A, Thr 90A, Thr 343F, Val 344F, Asp 345F, Glu 358F, Thr 359F, Ala 361F, Ala 362F, Thr 364F, Ile 570F, Gly 571F, Arg 579F, Val 580F, Gly 581F, Glu 582F, Val 583F, Val 584F, Leu 585F, Tyr 623F, Trp 651F, Gly 657F, Val 658F, Arg 659F, Pro 660F, His 661F, Val 662F, Val 663F, Trp 671F, Ala 672F, Ala 673F, Asn 678C, <u>**Val 687F**</u>***, Pro 689F, Phe 781F
2	Situated at the interface between the chain C and chains I and G of neighbour trimer.	**Arg 2G**, Leu 3G, Thr 4G, Pro 5G, His 6G, Gln 8G, Gln 354C, Val 357C, Glu 358C, Ala 361C, Gly 581C, Glu 582C, Val 658C, <u>Arg 659C</u>***, Pro 660C, <u>His 661C, Val 662C</u>, Val 663C, Trp 671C, Ala 672C, <u>Ala 673C</u>, Asn 678I, <u>**Val 687C**</u>, Leu 688C, Pro 689C, Arg 690C, Pro 691C, Phe 781C
3	Situated at the interface between the chain I and chain D of neighbour trimer.	Thr 4D, His 6D, Arg 10D, Thr 85D, Thr 90D, Thr 343I, Asp 345I, Glu 358I, Ala 361I, Ala362I, Thr 364I, Arg 579I, Val 580I, Gly 581I, Glu 582I, Val 583I, Val 584I, Leu 585I, Trp 651I, Gly 657I, Val 658I, <u>Arg 659I</u>, <u>Pro 660I</u>, Phe781I
4	Situated at the interface between chains C and A, and chains F and G of neighbour trimer.	**Met 1G, Arg 2G, His 32A**, Pro 33A, **Ile 36A**, Met 76A, *Leu 77A, Glu 79A, Val 80A, Gln 81A*, <u>Arg 337C</u>, Ile 351F, Cys 352F, <u>Pro 374F</u>, Ala375F, Arg 579F, <u>Glu 652C</u>, <u>Val 654C</u>, **Phe 655C**, <u>Arg 659C</u>, <u>His 661C</u>, Ala 672C, <u>Ala 673C</u>, Met 674C, Gly 675C, Asp 676C, Ala 677C, Ile 681C, <u>Pro 682C</u>, **Thr 683C**, <u>**Gln 685C**</u>, <u>**Val 687C**</u>, Met 692C, Arg 779C, Tyr 780C

* - Sites are numbered in accordance with the AlloPred's output. ** - Residues that coincide with (or equivalent to) residues of sites 1-3 identified by FTSite are highlighted in bold. *** - Residues that coincide with ones of ancillary pocket are underlined.

fulfill a very different function. Site 2 Consists of 28 residues of which 21 are common with site 0. It contains 2 residues which are equivalent with ones of FTSite's site 1 and 5 residue common with ancillary pocket. Site 3 comprises 24 residues of which 21 are common with site 0. It contains 2 residue common with ancillary pocket. Site 4 is located close to site 2 and partially overlaps with it. It

comprises 35 residues of which 7 are equivalent to ones of site 0 and 4 are common with site 2. Site 4 includes all residues of site 1 and all but one residues of site 2 revealed by FTSite server, and contains 13 residues common with ancillary pocket. Interestingly, AlloSite server predicted the single allosteric site
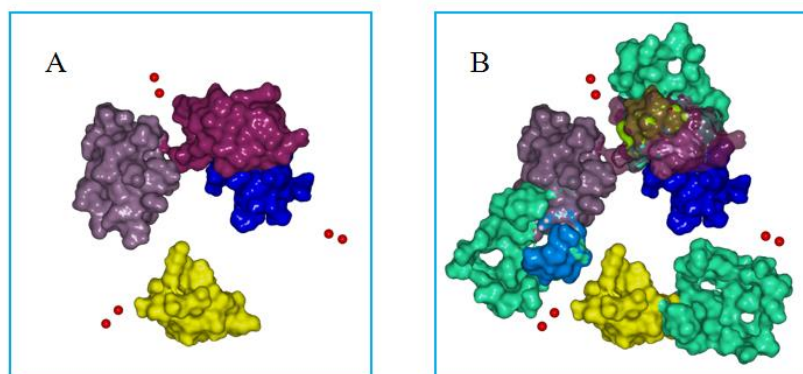
Fig. 8 - MTU binding sites identified by AlloPred. MTU structure is hidden for clarity. A – Binding sites and the active site's Ni atoms. B – Overlapping of binding sites identified by AlloPred and by FTSite, and the ancillary pockets. Ni atoms are colored in red. AlloPred's sites 0, 2, 3 and 4 are colored in amethyst-grey, blue, yellow and bordo, respectively. FTSite's sites 1, 2 and 3 are colored in pink, chartreuse-green and light-blue, respectively. Ancillary pockets are cyan colored.

(not shown) that completely coincides with AlloPred's site 0 (Table 2).

Thus, the MTU allosteric binding sites 0, 2, 3 and 4 predicted by AlloPred overlap with binding sites revealed by FTSite (partially in case of sites 0, 2 and 3 and almost completely in case of site 4) indicating their possible function as allosteric sites.

Conclusions

By computational solvent mapping method FTSite, we have explored *M.tuberculosis* urease nonamer surface to find sites that tend to bind small organic molecular probes representing fragments of drug molecules with diverse hydrophobic and hydrophilic properties. The predicted three top ranked binding sites were situated at the interfaces between chains C and A, and chain G of neighbour trimer (and at equivalent locations in symmetrical trimers as well). A mapping of enzymes generally yields the most probable sites situated in a subsite of the enzyme active site [28, 53, 54]. This was not the case for MTU which active sites were inaccessible for probes due to the closed conformation of the covering flap, and predicted binding sites were located not far from them at the entrance into a deep pocket. To explore their possible structural and functional role, we correlated the locations of predicted MTU binding sites and its ancillary pockets (which remain open and solvent exposed even while the flap is closed) and indicated their partial overlapping. This overlapping may suggest that predicted sites are likely the intermediate binding sites responsible for recruiting a ligand to another binding site deeply buried in the protein. Further, to examine the possibility that predicted binding sites are the sites for allostery binding we carried out the search for probable sites of allostery binding on MTU surface by AlloPred and AlloSite servers. Predicted probable allosteric sites overlapped with binding sites revealed by FTSite suggesting their possible function as sites for allosteric binding.

Taken together, on the surface of *M.tuberculosis* urease, there were revealed the probable ligand binding sites that appear to be the sites of allosteric binding. They may serve as promising targets for designing novel allosteric modulators as receptor-selective anti-tuberculosis drugs. The search for such modulators is underway in our laboratory.

References

1. WHO/HTM/TB2010.7 Pn. WHO Report 2010: Global Tuberculosis Control. Geneva, Switzerland: WHO Press; 2010.
2. Cole, S. T. Inhibiting *Mycobacterium tuberculosis* within and without [Text] / S. T. Cole // Phil. Trans. R. Soc. B. – 2016. – Vol. 371: 20150506.
3. Dixon, N. E. 1975. Jack bean urease (EC 3.5.1.5). A metalloenzyme. A simple biological role for nickel? [Text] / N. E. Dixon, C. Gazzola, R. L. Blakeley, B. Zerner. // J. Am. Chem. Soc. – 1975. – Vol. 97. – P. 4131–4133.
4. Ragsdale, S. W. Nickel-based enzyme systems [Text] / S.W. Ragsdale // J. Biol. Chem. – 2009. – Vol. 284, N 28. – P. 18571–18575.
5. Carter, E. L. Interplay of metal ions and urease [Text] / E. L. Carter, N. Flugga, J. L. Boer, S. B. Mulrooney, R. P. Hausinger // Metallomics. – 2009. – Vol. 1. – P. 207-221.
6. Boer, J. L. Nickel-dependent metalloenzymes [Text] / J. L. Boer, S. B. Mulrooney, R. P. Hausinger // Arch. Biochem. Biophys. – 2014. – Vol. 544. – P. 142-152.
7. Mobley, H. L. T. Molecular biology of microbial ureases [Text] / H. T. Mobley, M. D. Island, R. P. Hausinger // Microbiol. Rev. – 1995. – Vol. 59, N 3. - P. 451–480.
8. Mobley, H. L. T. Microbial ureases: significance, regulation, and molecular characterization [Text] / H. L. T. Mobley, R. P. Hausinger // Microbiol. Rev. – 1989. – Vol. 53, N 1. – P. 85–108.
9. Suzuki, K. Urease-producing species of intestinal anaerobes and their activities [Text] / K. Suzuki, Y. Benno, T. Mitsuoka, S. Takebe, K. Kobashi, J. Hase // Appl. Environ. Microb. - 1979. – Vol. 37, N 3. - P. 379-382.
10. Clemens, D. L. Purification, characterization, and genetic analysis of *Mycobacterium tuberculosis* urease, a potentially critical determinant of host-pathogen interaction [Text] / D. L. Clemens, B.-Y. Lee, M. A. Horwitz // J. Bacteriol. – 1995. – Vol. 177, N 19. – P. 5644-5652.
11. Dupuy, B. *Clostridium perfringens* urease genes are plasmid borne [Text] / B. Dupuy, G. Daube, M. R. Popoff, S. T. Cole // Infect. Immun. – 1997. – Vol. 65, N 6. – P. 2313-2320.
12. Tange, Y. Identification of the ure1+ gene encoding urease in fission yeast [Text] / Y. Tange, O. Niwa // Curr. Genet. – 1997. – Vol. 32, N 3. – P. 244-246.
13. Sirko, A. Plant ureases: roles and regulation [Text] / A. Sirko, R. Brodzik // Acta Biochim. Pol. – 2000. – Vol. 47, N 4. – P. 1189-1195.
14. Konieczna, I. Bacterial ureases and its role in long-lasting human diseases [Text] / I. Konieczna, P. Zarnowiec, M. Kwinkowski, et al. // Curr. Protein. Pept. Sci. – 2012. – Vol. 13. – P. 789-806.
15. McLean, R. J. C. The ecology and pathogenicity of urease-producing bacteria in the urinary tract [Text] / R. J. C. McLean, J. C. Nickel, K.-J. Cheng, J. W. Costerton // CRC Crit. Rev. Microbiol. – 1988. – Vol. 16, N 1. – P. 37–79.
16. Burne, R. A. Bacterial ureases in infectious diseases [Text] / R. A. Burne, Y.-Y. M. Chen // Microbes and Infection. – 2000. – Vol. 2. – P. 533−542.
17. Collins, C. M. Bacterial ureases: structure, regulation of expression and role in pathogenesis [Text] / M. Collins and S. E. F. D'Orazio // Mol. Microbiol. – 1993. – Vol. 9, N 5. P. 907–913.
18. Lv, J. Structural and functional role of nickel ions in urease by molecular dynamics simulations [Text] / J. Lv, Y. Jiang, Q. Yu. // J. Biol. Inorg. Chem. – 2011. – Vol. 16. – P. 125-135.
19. Roberts, B. P. Wide-open flaps are key to urease activity [Text] / B. P. Roberts, B. R. Miller, A. E. Roitberg, R. M. Merz // J. Am. Chem. Soc. – 2012. – Vol. 134. – P. 9934–9937.
20. Macomber, L. Reduction urease activity by interaction with the flap covering the active site [Text] / L. Macomber, M. S. Minkara, R. P. Hausinger, K. M. Merz // J. Chem. Inf. Model. – 2015. – Vol. 55, N 2. – P. 354-361.

21. Minkara, M. S. Molecular dynamics study of *Helicobacter pylori* urease [Text] / M. S. Minkara, M. N. Ucisik, M. N. Weaver, K. M. Merz, Jr. // J. Chem. Theory Comput. – 2014. – Vol. 10. – P. 1852-1862.

22. Clemens, D. L. Purification, characterization, and genetic analysis of *Mycobacterium tuberculosis* urease, a potentially critical determinant of host-pathogen interaction[Text] / D. L. Clemens, B. Lee, M. A. Horwitz // Journal of bacteriology. – 1995. – Vol. 177, N 19. - P. 5644–5652.

23. Modolo, L. V. An overview on the potential of natural products as urease inhibitors: a review [Text] / L. V. Modolo, A. X. de Souza, L. P. Horta, D. P. Araujo, A. de Fatima // J. Adv. Res. – 2015. – Vol. 6. – P. 35-44.

24. Azizian, H. Large-scale virtual screening for the identification of new Helicobacter pylori urease inhibitor scaffolds [Text] / H. Azizian, F. Nabati, A. Sharifi, F. Siavoshi, M. Mahdayi, M. Amanlou // J. Mol. Model. – 2012. – Vol. 18. – P. 2917–2927.

25. Ibrar A, Khan I, Abbas N. Structurally diversified heterocycles and related privileged scaffolds as potential urease inhibitors: a brief overview [Text] / A. Ibrar, I. Khan, N. Abbas // Arch. Pharm. Chem. Life Sci. – 2013. – Vol. 346. – P. 423–446.

26. Clark, G. C. The rational design of bacterial toxin inhibitors [Text] / G. C. Clark, A. K. Basak, R. W. Titball //Current Computer-Aided Drug Design. – 2007. – Vol. 3. – P. 1-12

27. Zhong, S. Computational identification of inhibitors of protein-protein interactions [Text] / S. Zhong, A. T. Macias, A. D. MacKerrel Jr. // Current Topics in Medicinal Chemistry. – 2007. – Vol. 7. – P. 63-83.

28. Silberstein, M. Identification of substrate binding sites in enzymes by computational solvent mapping [Text] / M. Silberstein, S. Dennis, III L Brown, T. Kortvelyesi, K. Clodfelter, S. Vajda // J. Mol. Biol. - 2003. – Vol. 332. – P. 1095-1113.

29. Lisnyak, Yu. Homology modeling and molecular dynamics study of *Mycobacterium tuberculosis* urease [Text] / Yu. V. Lisnyak, A. V. Martynov // Annals of Mechnikov Institute. – 2017. – N 3.

30. Benson, D. A. GenBank [Text] / D. A. Benson, I. Karsch-Mizrachi, D. J. Lipman, J. Ostell, D. L. Wheeler // Nucl. Acids Res. – 2007. – Vol. 35, Suppl 1. – P. D21-D25.

31. Altschul, S. F. Basic local alignment search tool [Text] / S. F. Altschul, W. Gish, W. Miller, E. W. Myers, D. J. Lipman // J. Mol. Biol. – 1990. – Vol. 215. - P. 403-410.

32. Altschul, S. F. Gapped BLAST and PSI-BLAST: a new generation of protein database search programs [Text] / S. F. Altschul, T. L. Madden, A. A. Schaeffer, J. Zhang, Z. Zhang, W. Miller, D. J. Lipman // Nucleic Acids Res. – 1997. – Vol. 25. - P. 3389-3402.

33. Rose, P. W. The RCSB protein data bank: integrative view of protein, gene and 3D structural information [Text] / P. W. Rose, A. Prlić, A. Altunkaya, C. Bi et al. // Nucleic Acids Research. – 2017. – Vol. 45. – P. D271-D281.

34. Hooft, R. W. W. Errors in protein structure [Text] / R. W. W. Hooft, G. Vriend, C. Sander, E. E. Abola // Nature. – 1996. – Vol. 381, N 6580. – P. 272-272.

35. Hooft, R. W. W. The PDBFINDER database: A summary of PDB, DSSP and HSSP information with added value [Text] / R. W. W. Hooft, C. Sander, G. Vriend // CABIOS/Bioinformatics. – 1996. – Vol. 12. – P. 525-529.

36. Mueckstein, U. Stochastic pairwise alignments [Text] / U. Mueckstein, I. L. Hofacker, P. F. Stadler // Bioinformatics. – 2002. – Vol. 18, Sup. 2. – P. 153-160.

37. Qiu, J. SSALN: an alignment algorithm using structure dependent substitution matrices and gap penalties learned from structurally aligned protein pairs [Text] / J. Qiu, R. Elber // Proteins. – 2006. – Vol. 62. – P. 881–891.

38. Canutescu, A. A. Cyclic coordinate descent: A robotics algorithm for protein loop closure [Text] / A. A. Canutescu, R. L. Jr. Dunbrack // Protein Sci. – 2003. – Vol. 12. – P. 963-972.

39. Canutescu, A. A. A graph-theory algorithm for rapid protein side-chain prediction [Text] / A. A. Canutescu, A. A. Shelenkov, R. L. Jr. Dunbrack // Protein Sci. – 2003. – Vol. 12. – P. 2001-2014.

40. Krieger, E. Assignment of protonation states in proteins and ligands: combining pKa prediction with hydrogen bonding network optimization [Text] / E. Krieger, R. L. Dunbrack, R. W. Hooft, B. Krieger // Methods Mol. Biol. – 2012. – Vol. 819. – P. 405-421.

41. Kreiger, E. Improving physical realism, stereochemistry, and side-chain accuracy in homology modelling: four approaches that perfomed well in CASP8 [Text] / E. Kreiger, K. Joo, J. Lee, et al. // Proteins. – 2009. – Vol. 77, Suppl. 9. – P. 114-122.

42. Ngan, C.-H. FTSite: high accuracy detection of ligand binding sites on unbound protein structures [Text] / C. H. Ngan, D. R. Hall, B. Zerbe, L. E. Grove, D. Kozakov, S. Vajda // Bioinformatics. – 2012. – Vol. 28, N 2. – P. 286-287.

43. Kozakov, D. The FTMap family of web servers for determining and characterizing ligand-binding hot spots of proteins [Text] / D. Kozakov, L. E. Grove, D. R. Hall, T. Bohnuud et al // Nature Protocols. – 2015. – Vol. 10, N 15. – P. 733-755.

44. Brenke, R. Fragment-based identification of druggable "hot spots" of proteins using Fourier domain correlation techniques [Text] / R. Brenke, D. Kozakov, G.-Y. Chuang, D. Beglov, D. Hall, M. R. Landon, C. Mattos, S. Vajda // Bioinformatics. – 2009. – Vol. 25. – P. 621–627.

45. Landon, M. R. Identification of hot spots within druggable binding sites of proteins by computational solvent mapping [Text] / M. R. Landon, D. R. Lancia Jr, J. Yu, S. C. Thiel, S. Vajda S // J. Med. Chem. – 2007. – Vol. 50. – P. 1231-1240.

46. Greener, J. G. AlloPred: prediction of allosteric pockets on proteins using normal mode perturbation analysis [Text] / J. G. Greener, M. J. E. Sternberg // BMC Bioinformatics. – 2015. Vol. 16, N335. – P. 1-7.

47. Hayward, S. Normal modes and essential dynamics [Text] / S. Hayward, B. L. de Groot // Methods Mol. Biol. – 2008. – Vol. 443. – P. 89–106.

48. Le Guilloux, V. Fpocket: An open source platform for ligand pocket detection [Text] / V. Le Guilloux, P. Schmidtke, P. Tuffery // BMC Bioinformatics. – 2009. – Vol. 10, N 168. – P. 1–11.

49. Tirion, M. M. Large amplitude elastic motions in proteins from a single-parameter, atomic analy sis [Text] / M. M. Tirion // Phys. Rev. Lett. - 1996. – Vol. 77, N 9. – P. 1905–1908.

50. Huang, W. Allosite: a method for predicting allosteric sites [Text] / W. Huang, S. Lu, Z. Huang, X. Liu X, et al. // Bioinformatics. – 2013. – Vol. 29, N 18. – P. 2357-2359.
51. Christopoulos, A. G protein-coupled receptor allosterism: the promise and the problem(s) [Text] / A. Christopoulos, L. T. May, V. A.Amani, P.M. Sexton // Biochem. Soc. Transactions. – 2004. – Vol. 32, N 5. – P. 873-877.
52. May, L. T. Allosteric modulation of G protein-coupledreceptors [Text] / L. T. May, K. Leach, P. M. Sexton, A. Christopoulos // Annu. Rev. Pharmacol.Toxicol. – 2007. – Vol. 47. – P. 1-51.
53. Kortveyesi, D. S. Computational mapping identifies the binding sites of organic solvents on protein [Text] / D. S. Kortveyesi, S. Vajda // Proc. Natl. Acad. Sci. U.S.A. – 2002. – Vol. 99. – P. 4290-4295.
54. Silberstein, M. Exploring the binding sites of the haloalkene dehalogenase DhlA from *Xanthobacter autotrophicus* GJ10 [Text] / M. Silberstein, J. Damborsky, S. Vajda // Biochemistry. – 2007. – Vol. 46. – P. 9239-9249.

**LIGAND-BINDING SITES ON THE
MYCOBACTERIUM TUBERCULOSIS UREASE**
Lisnyak Yu. V., Martynov A. V.
Introduction. *Mycobacterium tuberculosis* is the causative agent of tuberculosis that remains a serious medical and social health problem. Despite intensive efforts have been made in the past decade, there are no new efficient anti-tuberculosis drugs today, and that need is growing due to the spread of drug-resistant strains of *M.tuberculosis*. *M. tuberculosis* urease (MTU), being an important factor of the bacterium viability and virulence, is an attractive target for anti-tuberculosis drugs acting by inhibition of urease activity. However, the commercially available urease inhibitors are toxic and unstable, that prevent their clinical use. Therefore, new more potent anti-tuberculosis drugs inhibiting new targets are urgently needed. A useful tool for the search of novel inhibitors is a computational drug design. The inhibitor design is significantly easier if binding sites on the enzyme are identified in advance. This paper aimed to determine the probable ligand binding sites on the surface of *M. tuberculosis* urease. **Methods.** To identify ligand binding sites on MTU surface, computational solvent mapping method FTSite was applied by the use of MTU homology model we have built earlier. The method places molecular probes (small organic molecules containing various functional groups) on a dense grid defined around the enzyme, and for each probe finds favorable positions. The selected poses are refined by free energy minimization, the low energy conformations are clustered, and the clusters are ranked on the basis of the average free energy. FTSite server outputs the protein residues delineating a binding sites and the probe molecules representing each cluster. To predict allosteric pockets on MTU, AlloPred and AlloSite servers were applied. AlloPred uses the normal mode analysis (NMA) and models how the dynamics of a protein would be altered in the presence of a modulator at a specific pocket. Pockets on the enzyme are predicted using the Fpocket algorithm.

To model the reduction in flexibility of allosteric pocket on modulator binding, the unperturbed normal modes are first calculated for the protein. The calculation is then repeated, each time perturbing one of the pockets in the protein. These results are combined with output from Fpocket in a support vector machine (SVM) to predict allosteric pockets on proteins. The AlloSite server is similar to the AlloPred method in that it uses the Fpocket algorithm to elucidate allosteric pockets, whereas AlloPred uses an approach that combines flexibility with the Fpocket output. **Results and discussion.** By computational solvent mapping method FTSite, we have explored *M.tuberculosis* urease nonamer surface to find sites that tend to bind small organic molecular probes representing fragments of drug molecules with diverse hydrophobic and hydrophilic properties. The predicted three top ranked binding sites were situated at the interfaces between chains C and A, and chain G of neighbour trimer (and at equivalent locations in symmetrical trimers as well). A mapping of enzymes generally yields the most probable sites situated in a subsite of the enzyme active site. This was not the case for MTU which active sites were inaccessible for probes due to the closed conformation of the covering flap, and predicted binding sites were located not far from them at the entrance into a deep pocket. To explore their possible structural and functional role, we correlated the locations of predicted MTU binding sites and its ancillary pockets (which remain open and solvent exposed even while the flap is closed) and indicated their partial overlapping. This overlapping may suggest that predicted sites are likely the intermediate binding sites responsible for recruiting a ligand to another binding site deeply buried in the protein. To examine the possibility that predicted binding sites are the sites for allostery binding we carried out the search for probable sites of allostery binding on MTU surface by AlloPred and AlloSite servers. Predicted probable allosteric sites overlapped with binding sites revealed by FTSite suggesting their possible function as sites for allosteric binding. **Conclusions.** On the surface of *M.tuberculosis* urease, there were revealed the probable ligand binding sites that appear to be the sites of allosteric binding. They may serve as promising targets for designing novel allosteric modulators as receptor-selective anti-tuberculosis drugs.

Key words: *Mycobacterium tuberculosis* urease, anti-tuberculosis drugs, allosteric binding, computational drug design.